Flight Performance of TOPEX/POSEIDON Star Trackers

David J. Flynn, Walter J. Fowski

Hughes Danbury Optical Systems, Inc.
100 Wooster Heights Road, Danbury, Connecticut 06810-7S89

Tooraj Kia

Jet Propulsion Laboratory
California Institute of Technology, Pasadena, California 91109

ABSTRACT

The TOPEX/POSEIDON spacecraft was launched on August 10, 1992. This paper will present data on the measured performance of the ASTRA Star Trackers supplied by 1 lughes Danbury Optical Systems (HDOS) for this satellite.

The 1 HDOS ASTRA Star Tracker is a charge coupled device (CCD), microprocessor based replacement for the NASA Standard Fixed Head Star Tracker. The position and magnitude accuracy of the star trackers computed from measured flight data will be compared with ground measurements and system models.

The performance of novel transient rejection algorithms implemented in the ASTRA Star Tracker which allows uninterrupted operation in the South Atlantic Anomaly (SAA) where the sensor is subjected to high proton flux levels, will also be presented.

1. MIS SION OVERVIEW

The TOPEX/POSEIDON remote sensing mission is a scientific program sponsored jointly by the U.S. National Aeronautics and Space Administration (NASA) and the French Centre National d'Etudes Spatiales (CNES). This U.S./French project combines each agencies ocean rc.search activities. The TOPEX project is being managed by the Jet Propulsion Laboratory (JPL) for the NASA office of Space Science and Application. CN1X'S"I6U1OUSC Space Laboratory is managing the POSEIDON project.

TOPEX/POSEIDON is a dedicated altimetry mission that introduces major advances in measurement accuracy[1]. It uses a state-of-the-art dual-frequency radar altimeter along with a microwave radiometer for correction of the altimeter measurements, and high-accuracy satellite orbit determination using Global Positioning System (GPS) and Determination of Orbit Radiopositioning Integrated from Satellite. (DORIS) measurements.

TOPEX/POSEIDON will increase understanding of ocean dynamics by collecting accurate and long term observations of the global sea levels. The mission has been planned for a three year life with a possible extension to five years. The TOPEX/POSEIDON mission will coordinate with two other major world research programs: The World Ocean Circulation Experiment (WOCE) and the Tropical Oceans and Global Atmosphere (TOGA) program. Some of the major science goals of the mission arc the following:

- Determination of the general circulation of the ocean and its variability through combining sea level internal density field measurements of the ocean and models of ocean circulation.
- Description of the nature of ocean dynamics.
- Calculation of the transport of heat, mass, nutrients, and salt by the oceans.
- Investigation of the. geocentric ocean tides, and improving the knowledge of the marine geoid.

. Investigation of the interaction of currents with waves.

These goals, in turn, resulted in a set of science/mission requirements. The primary requirement being geocentric global ocean sea level measurements with a precision of ± 2.4 cm and an accuracy of ± 14 cm, along a fixed ground track. The tracks arc to be repeated every ten days for the duration of the mission, Both precision orbit determination (POD) and the satellite pointing requirements were derived from this primary requirement.

2, SATELLITE DESCX1FI'1ON

Fairchild Space Company was selected as the prime contractor responsible for the design, development, integration, test, and launch of the TOPEX/POSEIDON satellite under contract to JPL.

The TOPEX/POSEIDON satellite is an Earth pointing, three axis body stabilized spacecraft based on NASA'S Multi-Mission Satellite (M MS) design, as illustrated in Fig. 1. The satellite is maintained in a nearly circular high inclination non-synchronous orbit as shown in Table 1. This orbit was selected to minimize the geophysical impact on the precision orbit determination. A characteristic of this orbit is its high radiation content. To ensure at least three years of life, the satellite had to be designed to a 72 Krad total dose, with capability to recover from highly probable single. event upsets (SEU). A contour map of the high energy proton ftux environment for the TOPEX/POSEIDON is shown in Fig. 2.

3. ATTITUDE D ETERMINATION AND CONTROL SUBSYSTEM

The TOPEX/POSEIDON Attitude Determination and Control Subsystem (ADCS) consists of a modular attitude control subsystem (MACS) module ancf digital on-board computer (OBC). The ADCS contains all equipment required for attitude stabilization, acquisition, determination, and control. Built-in redundancy in the ADCS design provides flexibility in case of component failures.

A layout drawing of the Fairchild MACS module is shown in Fig. 3[2]. The satellite attitude control equipment consists of four reaction wheel assemblies (RWA), four magnetic torque. bars (MTB) and attitude thrusters. The attitude sensors consists of a dry rotor inertial refe rence unit (DRIRU-II), two solid state. fixed head ASTRA Star Trackers, one digital firm sun sensor (DFSS), two tri-axis magnetometers (TAM), an externally mounted, nadir pointing, Earth sensor assembly module (ESAM), and externally mounted course sun sensors. The star trackers and the inertial sensor (DRIRU-II) are mounted on a thermally and mechanically stable optical bench.

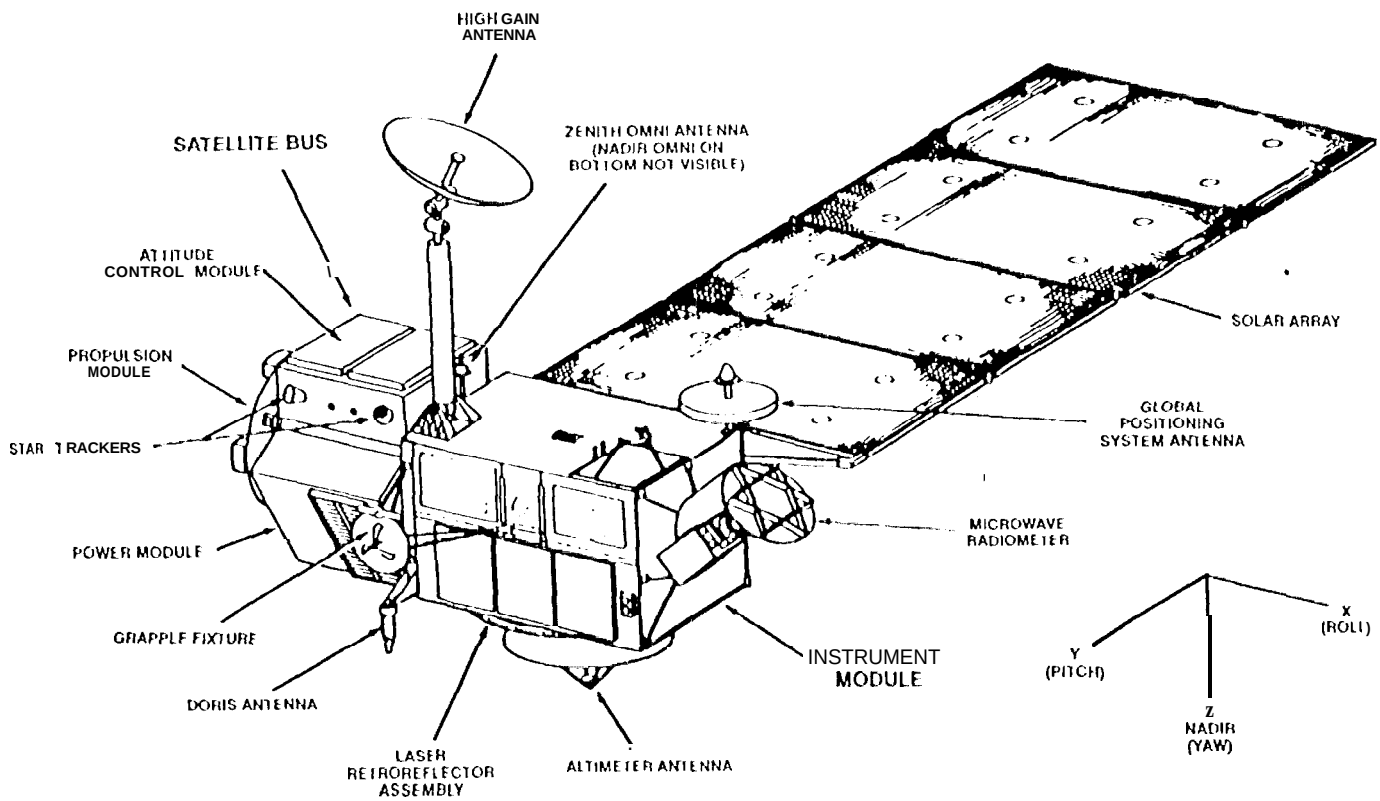

Fig. 1. TOPEX/POSEIDON spacecraft.

Table 1. TOPEX/POSEIDON Operational Orbit

Orbit Parameter	Value
Altitude	1335 Km
Inclination	66°
Eccentricity	< 0.0010
Nodal Period	112.4 minutes
Ascending, Node Crossings	12.7 revs/day
Ascending Node Longitude Increments	28.35°
Repeat cycle	9.91 days (127 revs)
Ground Cross 'Track Repeatability at Equator	* 1.0 Km

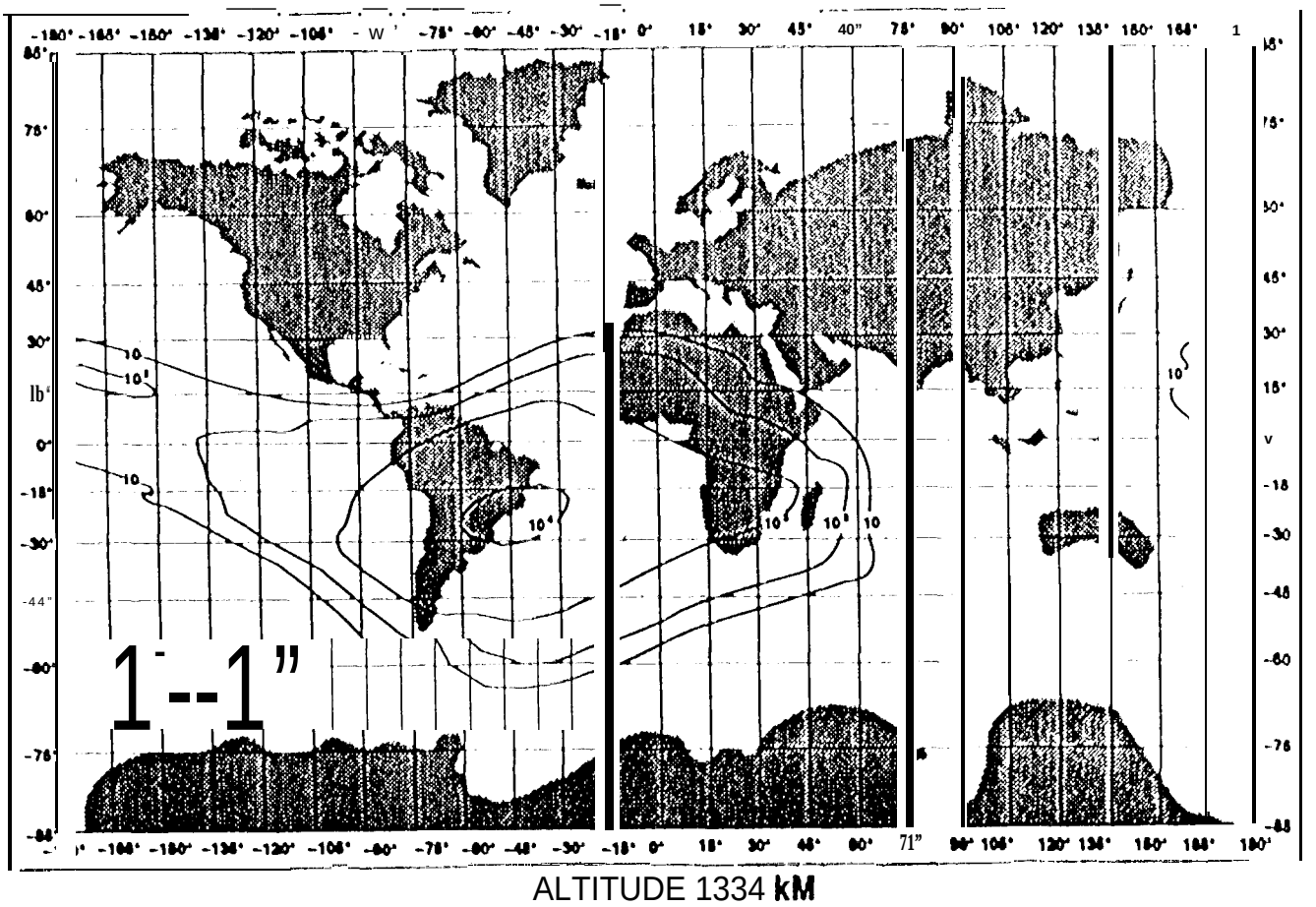

Fig. 2. TOPEX/POSEIDON Star Tracker is required to operate in a severe radiation environment.

The TOPEX/POSEIDON attitude determination system employs a stellar-inertinl technique. similar to the one flown on previous MMS missions[3]. The high performance. inertial measurement device, DRIRU-II, is used for short term relative attitude measurements and the star sensor, or digital fine sun sensor, provides periodic absolute measurement updates.

An on-board six state Kalman filter recursive estimator provides estimates of the gyro drift rate and spacecraft attitude in all axes.

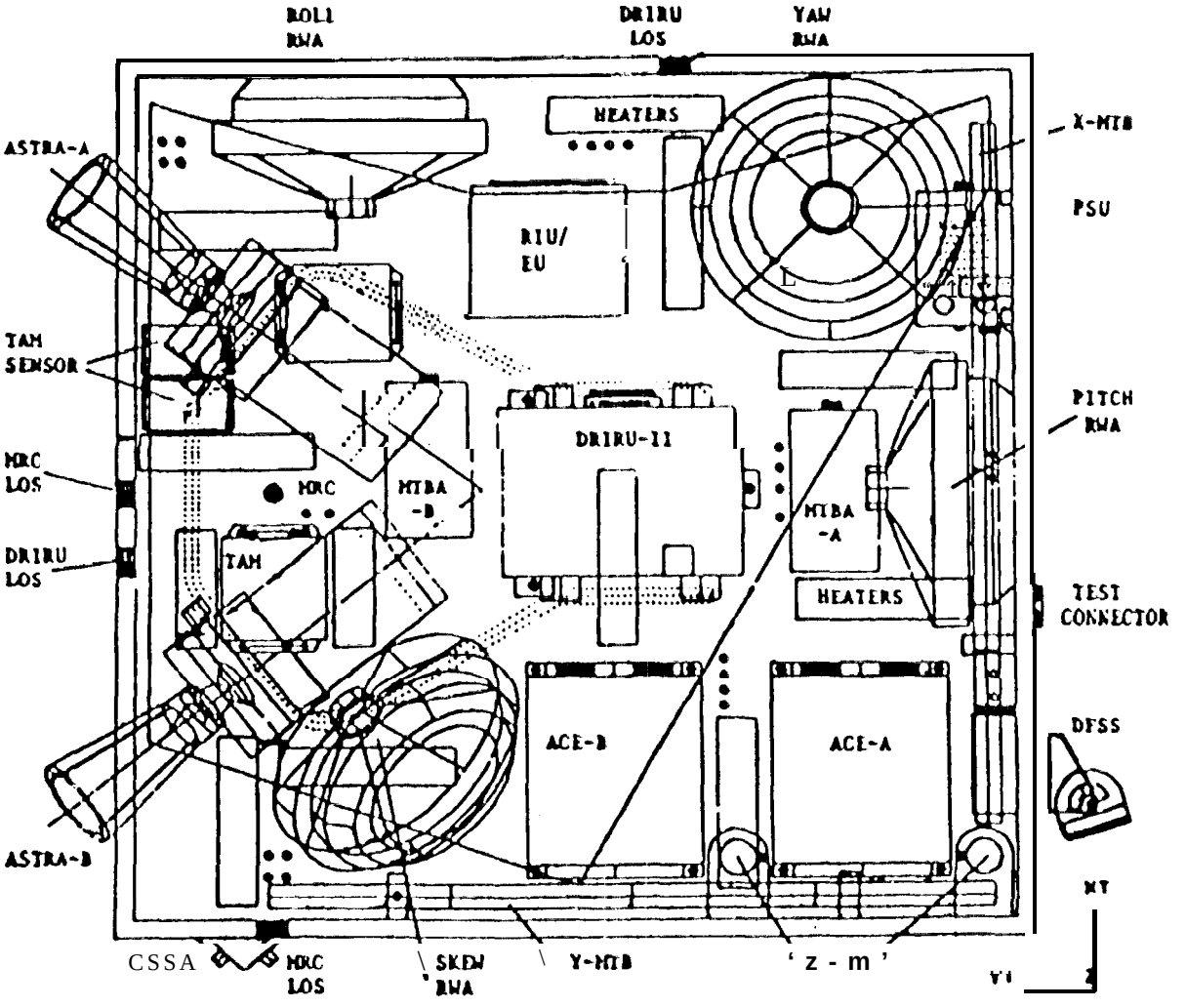

Fig. 3. Fairchild's MMS MACS module.

Fundamental pointing requirement for the satellite was defined as the ability to point the satellite Z-axis to the local nadir, as defined by a reference ellipsoid, to within 0.08° (0.05°) control (knowledge) 1σ accuracy. This requirement was further broken down into error allocations for the orbit determination, structural, and attitude error budgets. Table provides the normal mission mode attitude determination error allocations, and its breakdown into internal ADCS components.

4. ASTRA STAR TRACKER

The ASTRA Star Tracker, developed by Hughes Danbury Optical Systems, is a CCD, microprocessor based replacement for the NASA Standard Fixed Head Star Tracker. The ASTRA sensor uses a 256x403 pixel, RCA 504 CCD array. This thinned backside illuminated device provides high quantum efficiency in the visible range. A thermoelectric cooler is used to reduce CCD dark current. This is necessary since the dark current of the device will rise over life in the. harsh radiation environment[4].

The ASTRA Star Tracker is fitted with a wide field of view (7° x9"), f/1.6 lens. The lens is color corrected to reduce position error due to star color temperature, In order to meet the accuracy requirements the lens was designed to minimize residual geometric distortion and to maintain a constant spot size throughout the field of view. Thermal stability of the lens cell and focal plane was also required to meet accuracy requirements. Due to the severe radiation environment, radiation hard glass was used to reduce radiation darkening of the glass over life.

Table 2. Attitude Determination Error Budget

Error Source	Roll (arcsec 1σ)	Pitch (arcsec 1σ)	Yaw (arcsec 1σ)
Star Location Uncertainty	4.0	4.0	4.0
Chromatic Aberration Error	10.0	10.0	10.0
Kalman Filter Residuals	20.0	20.0	20,0
ASTRA Optical Axis Uncertainty	5.0	5.0	5.0
Total (RSS)	23.3	23.3	23.3
Requirement	54.0	54.0	252.0

The ASTRA star sensor uses a versatile 16-bit microprocessor. A software "state machine." controls the. hardware and software.required to drive the CCD, process the CCD data, and perform diagnostic functions. A mixture of hardware and software is used to process the large amount of data generated by the CCD at the 10117 update rate. Correlated double sampling, analog-to-digital (A/D) conversion, and high pass filtering are performed in hardware. Acquisitiem and tracking, centroid determination and correction, debris and transient event discrimination, and self-test functions are all performed autonomously by the microprocessor reducing computational burden on the. host computer.

s. SUMMARY OF ON-ORBIT OPERATI ONS

On August 10, 1992 the TOPEX/POSEIDON satellite was launched from Kourou, French Guiana, aboard an Ariane 42P launch vehicle. The sate.llitc achieved its proper orbit and all appendages, antennae and solar array, deployed as planned.

Early in the. mission the effects of the severe radiation environment on the sensors aboard the satellite became apparent[5]. On November 26, 1992. the. AS'I'ILA-l{Star 3tackcr entered an anomalous mode and no longer tracked stars. This anomaly is discussed in more detail in the next section. It should be noted that due to the built-in redundancy of the ADCS design, all attitude determination requirements are still being met.

On December 8, 1992 the initial system calibrations were completed permitting the collection of accurate science data. Further fine calibration of the attitude sensors is continuing on a noninterference basis with the collection of science data[6]. On December 16,1992 an adjustment to the magnitude threshold level was implemented which incrcascd the probability of the OBC identifying a star, this will be discussed in more detail later in the paper. On February 26, 1993 the science verification workshop completed its favorable evaluation of system performance..

6. ASTRA-B ANOMALY

On November 26,1993, after 108 days of satisfactory operation, the ASTRA-B Star Tracker ceased to track identifiable stars while passing through the South Atlantic Anomaly, After onc orbit of unsuccessful star identification efforts, an on-board failure detection and correction routine issued an SEU re.set command which initiated a star tracker self test sequence, closing the shutter, turning off the thermoelectric cooler (TEC) and performing various memory and logic checks.1'hc tracker failed to exit the self test sequence and remained hung-up in ashuttcr-closed,'I'i i~;-offmoclc. Once the shutter is closed, the tracker will remain in a perceived bright object (BO) state and will queue further command inputs until the perceived BO is gone. Therefore, the only control available to ground personnel was to issue additional SEU reset commands (which initiated the hung-up condition) or power cycle the tracker, an option considered to be of some risk to future mission operations. An extensive review of pre and post anomaly data was conducted to gain insight into the status of the tracker, to determine what caused the anomaly, and to assess the probability of success by power cycling or other ground controlled actions.

The star tracker data available was initially limited to one sample every four seconds. Therefore, most of the S/W status information output by the tracker at a 10 Hz rate was not available for analysis. Prior to the failure, the most useful data was the background information, output as a result of a BO search which is normally conducted when attempting to acquire a ncw star. Figure 4 provides the background data prior to and after the on-orbit anomaly. The total background, in A/f) converter counts, is the sum of counts from 19S pixels in a 13 x 15 pixel patch which is used to detect a bright object. Figure 4 shows a normal background of approximately 6000 to 8000 counts prior to the anomaly and an abnormal background of approximately 16000 to 18000 counts immediately after the anomaly. Upon receipt of the SEU reset command, we see the

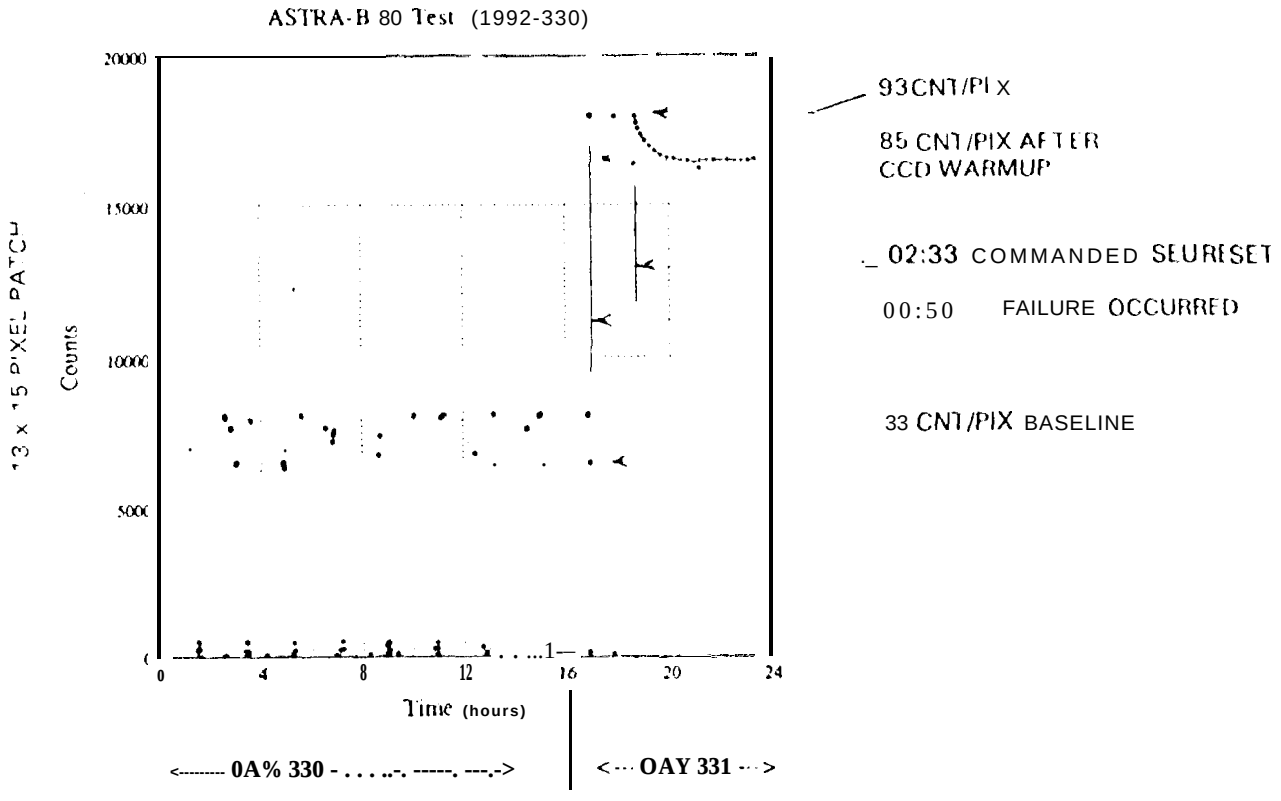

Fig. 4. Description of conditions at time of failure.

effect of the shutter closing and an initially perplexing (wrong polarity) exponential decay. Further evaluation of CCD dark current noise and dark current variation with temperature (Fig. 5) after the failure provided evidence that the CCD and most of its signal processing electronics were operating normally. However, data from a moon passage through the FOV on December 1, 1992 (Fig. 6) provided the clue which led to an understanding of the failure mode. Note that this moon passage generates lower background counts than the absence of the moon. This signature plus the inverted exponential decay in Fig. 4 and the 180° phase shift between dark current and CCD temperature pointed to an inversion in the processing of CCD data and, ultimately, the identification of a mode change in the A/D converter output as the cause of the anomaly.

The AD9048 A/D converter can output data in one of four modes depending upon the state of the NLINV and NMINV inputs (as shown in Table 3). The ASTRA star tracker hardwires the AD9048 to provide a binary output. At the time of failure, the AD9048 switched to an inverted offset twos complement output state which, in addition to providing an inversion, provides an offset of 127 counts. This explains the inversion seen in the exponential decay when the TEC was turned off, the 180° phase shift in CCD dark current with temperature variation, and the reduction in background counts with moon passage. It also explains why the normal background level of ≈ 6000 counts (33 counts/pixel) jumped to ≈ 18000 counts (93 counts/pixel) at the time of failure. Confirmation of this analysis was received on January 3, 1993 when a brighter moon passage took place (Fig. 7) resulting in:

- The expected reduction in counts as the moon illuminates the 13 x 1S background patch of the CCD.
- Opening of the shutter when the count is low enough to indicate no BO is present,
- Execution of a TEC-on command in queue, the cool-down of the CCD, and an inverted profile of dark current reduction with CCD temperature change.
- Closing the shutter due to a perceived BO as the moon transitioned the FOV and the input to the A/D converter exceeded 1 volt.

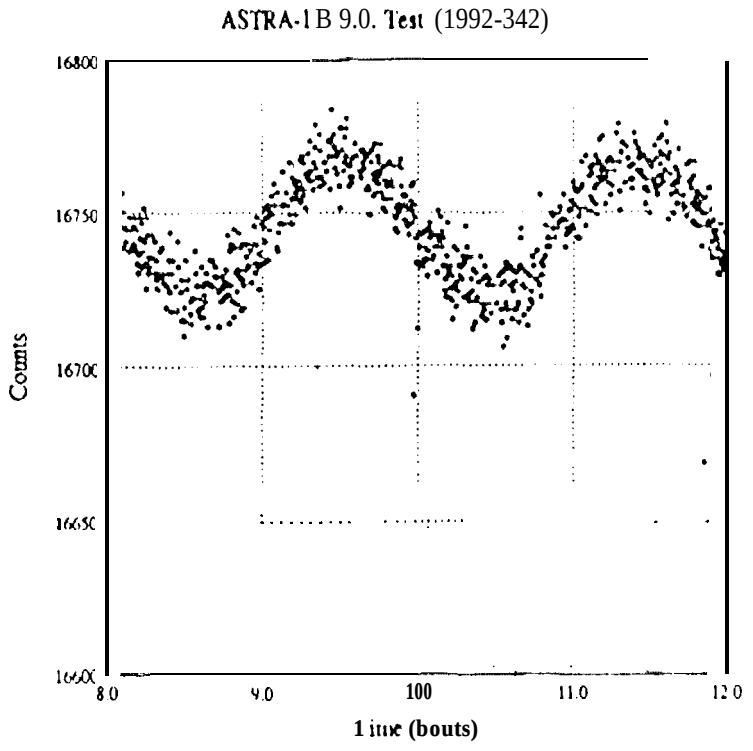

I_{OK} SHIFT IS CONSISTENT WITH CCD WARMUP OF 35° C AFTER INVERSION.

I_{DK} AMPLITUDE AND PHASING VARIATION IS CONSISTENT WITH 0.3° C ORBITAL TEMPERATURE VARIATION AFTER INVERSION.

NOISE IS CONSISTENT WITH ORIGINAL CCD CHARACTERIZATION DATA.

Fig. 5. Verification of detector health.

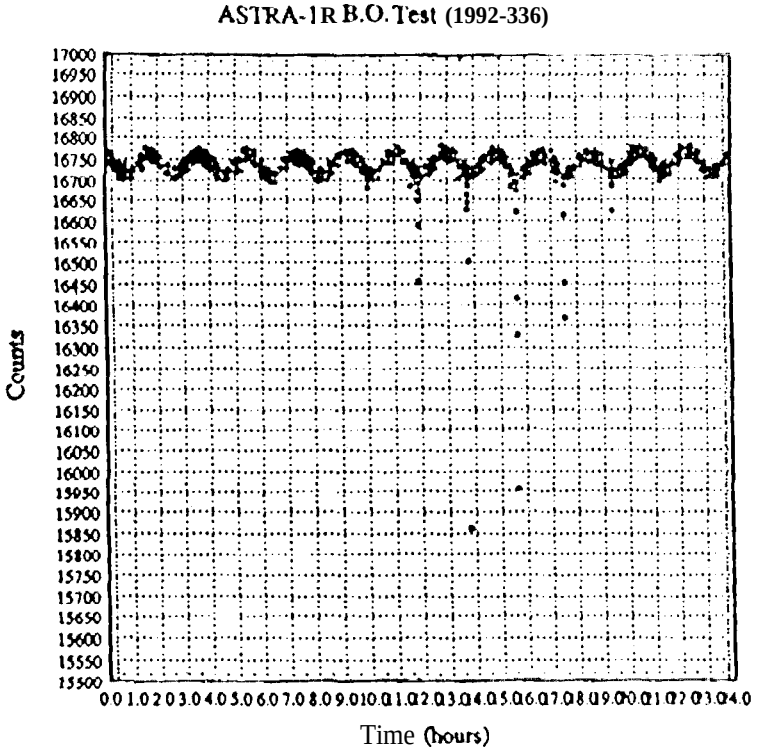

ASTRA 1-B LOCKED-UP WITH HIGH f3ACKGROUND COUNT

MOON ILLUMINATED SHUTTER PIN HOLES

BO COUNTS DECREASED WITH INCREASING LUNAR ILLUMINATION

ALL OTHER CHARACTERISTICS SEEMED NORMAL

SEARCH FOR INVERTED MODE OPERATION IDENTIFIED A/D CONVERT FAILURE MODE

Fig. 6. Failure mode breakthrough.

Table 3. AD9048 Truth Table

Step	Range		Bins True	Bins Inverted	Offset Twos Complement True	Offset Twos Complement Inverted
	2.000V FS	- 2.0480V FS	NMINV = 1	0	0	1
	7.8431mV Step	8.000mV Step	NLINV = 1	0	1	0
Ooo	0.0000V	0.0000V	00000000	11111111	10000000	01111111
001	- 0.0078V	0.0080V	00000001	11111110	10000001	01111110
.	.	.	.	.	.	.
.	.	.	.	.	.	.
.	.	.	.	.	.	.
127	- 0.9961V	- 1.0160V	01111111	10000000	11111111	00000000
128	1.0039V	- 1.0240V	10000000	01111111	00000000	11111111
129	- 1.0118V	- 1.0320V	10000001	01111110	00000001	11111110
.	.	.	.	.	.	.
.	.	.	.	.	.	.
.	.	.	.	.	.	.
254	- 1.9921V	- 2.0320V	11111110	00000001	01111110	10000001
255	- 2.0000V	- 2.0400V	11111111	00000000	01111111	10000000

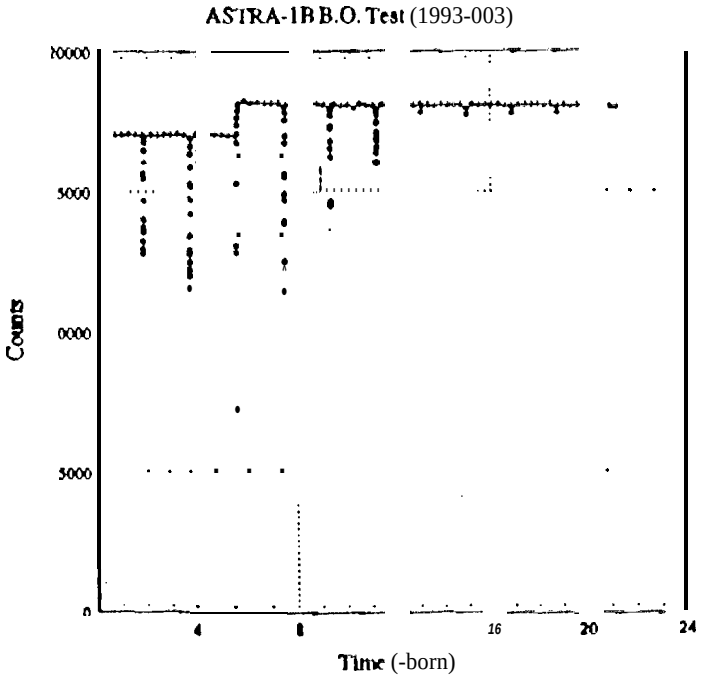

WHEN BACKGROUND DROPPED BELOW 9750 COUNTS, SH OPENED FOR 49 SECONDS

COMMANDS IN QUEUE WERE EXECUTED (TEC ON)

SH CLOSED - PROBABLY DUE TO A/D ROLLOVER AND BACKGROUND >39000 CNTS

CCD COOLED TO SETPOINT (-1°C)

CHANGE IN CCD I_{DK} AS EXPECTED

POWER SUPPLY TEMPERATURE INCREASED 3°C REFLECTING ADDED TEC POWER LOAD

Fig. 7. Bright moon passage on day 003 confirms theory.

At this time the cause of the anomaly remains unknown. A random part failure is possible. However, the coincidence of the failure with a 13 minute pass through the South Atlantic anomaly also points to a possible single event latch-up (SEL) of a non-destructive nature.}~causc the A/I) converter continues to output correct data but in the wrong format, there is strong support for an attempted recovery by power cycling. JPL's TOPEX Project Office is currently evaluating the risks associated with power cycling the "B" star tracker. At this time, successful operation of the mission continues using the "A" star tracker and other sensors for attitude determination.

7. ASTM-A PERFORMANCE ASSESSMENT

Table 4 lists the key performance requirements for the ASTRA Star Trackers.

All of the requirements above were verified durinp.the acceptance testing of the ASTRA Star Trackers[7]. These results will be compared to estimates of the pc rformance of the sensor based on on-orbit data.

Table 4. Star Tracker Performance Requirements

Parameter	Requirement (Beginning of Life)
Update Rate	10 Hz
10S Motion of Stars	< 0.3 degree/second
Accuracy Relative to Boresight	16.6 arcsec 10 (rnv S GOV, -20° C, +40°C)
Boresight Stability	< 120 arcscc peak (-20°C, +40°C)
Magnitude Accuracy at Boresight	±0.25 magnitude (mv2 to mv5)
Power	< 2.S watts (peak)
Weight	< 20 lbs
Radiation Tolerant, including proton events	(See Section 7.5)

7.1. Accuracy with respect to boresight: ground results

Since star sensor data is used for attitude determination, position accuracy is one of the key performance metrics. For the ASTRA Star Trackers, accuracy was broken down into two components, boresight stability and accuracy with respect to boresight.

Errors in the knowledge of the boresight of the star tracker relative to the spacecraft reference coordinates will result in a bias error in the reported position of a star in spacecraft coordinates. Boresight errors can result from a number of sources, errors in the. knowledge of the star tracker mounting surfaces relative to the spacecraft coordinates and bias errors in the star tracker reported position relative to the star tracker mounting surfaces. From the TOPEX telemetry data all that can be determined is the relative orientation of the attitude sensors with respect to onc another and wc cannot directly determine the stability of the ASTRA bore.sight. The calibration and stability of the attitude sensors with respect to one. another is discussed in reference 6.

Accuracy with respect to boresight includes all errors in the reported position of the star relative to the estimated position of the star with respect to the star tracker coordinate system. These errors can be divided into temporal errors and spatial errors.'lbmporal errors are defined as the standard deviation of the reported position of a star image that remains fixed in star tracker coordinates. Temporal position errors are. usually referred to as Noise Equivalent Angle (NEA). Shot noise, both from signal and background, and noise in the analog electronics contribute to NEA.

Spatial errors can be broken down into high and low spatial frequency components. Low spatial frequency errors arc usually systematic errors that can be calibrate.d and corrected. For example, error in the knowledge of the geometric effective focal length of the sensor will result in a plate scale (magnification) error. High spatial frequency errors can have both random and systematic components and in general cannot be calibrated. For example, random nonuniformities in the CCD responsivity and systematic quantization errors contribute to the high spatial frequency error of the sensor.

Figure 8 showsa typical vector plot of the residual errors measured during the ASTRA-A Star Tracker acceptance testing. The outer box indicates the bounds of the field of view, 7° x9 °. The error vectors are magnified and the "I" shaped symbol in the upper left corner provides the scale, 10 arcsec per axis. During this test the star tracker was mounted in a two-axis gimbal which allowed us to position the star image. throughout the total field of view. The gimbal would stop and 100 samples of tracker data was collected at each position in the "raster" pattern.'I'his allowed us to measure the NEA at each field position and decouple the spatial and temporal errors. As can be seen from the vector plot, there was some residual plate. scale error in the ASTRA-A tracker resulting from a minor rework of the. focal plane after the sensor was calibrated. The residual error in the plot shows< 6.5 arcsec 1σ per axis spatial error, and < 5.0 arcsec 1σ per axis NEA.

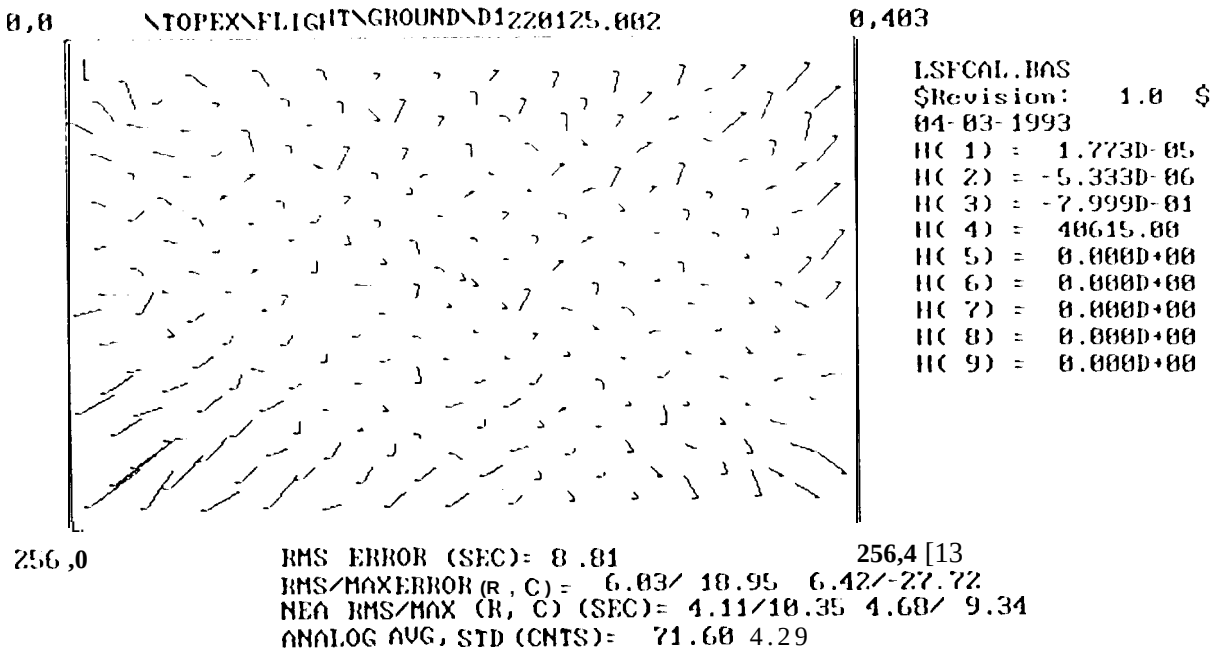

Fig. 8. Position accuracy: ground test results.

The ASTRA Star Trackers were extensively tested during acceptance. All accuracy tests were performed in vacuum over a temperature range from -20°C to 40°C. A polychromatic source was used to provide a realistic simulated star image during performance testing. The measured accuracy with respect to boresight, over all test environments, was < 12.5 arcsec 1σ per axis.

7.2, **Accuracy with respect to boresight: on-orbit results**

In order to determine position accuracy a reference is required against which to compare the measured on-orbit data. A direct measurement of the absolute position of a star with respect to star tracker coordinates is not available. In order to obtain an estimate of the actual position of a star, data from the star tracker, digital fine sun sensor and the inertial reference unit are combined over a period of time and an optimal post-facto estimate of the star position is found. In order to combine data from the different attitude sensors the alignment between the sensors must be known and the gyro bias and drift rates must also be estimated. Figure 9 shows the residual errors between a post-facto estimate of the star position and the reported position of the star for a typical orbit[6]. It should be noted that this data includes errors in the post-facto estimate; no attempt has been made to determine the magnitude of this error at this time. A conservative estimate of the peak position error based on this data is < 40 arcsec. At this time no attempt has be made to break the error down into the temporal and low/ high spatial frequency components.

73. Magnitude bias errors

Errors in the reported magnitude of a star can be divided into bias errors and stability errors over the sensor field of view. The star tracker cannot determine the color of a star so it reports the instrument magnitude of the star which is independent of color[8]. In order to compute the instrument magnitude of a star one needs to know the spectral response of the instrument, the spectral irradiance of the star, and the spectral irradiance of the "zero point" star. Errors in the knowledge of the relative spectral response of the star tracker or in the relative spectral irradiance of a star will result in color dependent magnitude bias errors. Errors in the knowledge of the absolute spectral response of the tracker or in the absolute irradiance of a star will result in color independent bias errors. The ASTRA Star Tracker is required to track stars over a wide dynamic range. The response of the tracker becomes nonlinear at the upper end of the dynamic range due to saturation of the 8-bit A/D converter and nonlinear at the lower end due to truncation and thresholding. Errors in the calibration of these nonlinearities can result in magnitude dependent bias errors. The estimated bias error in the

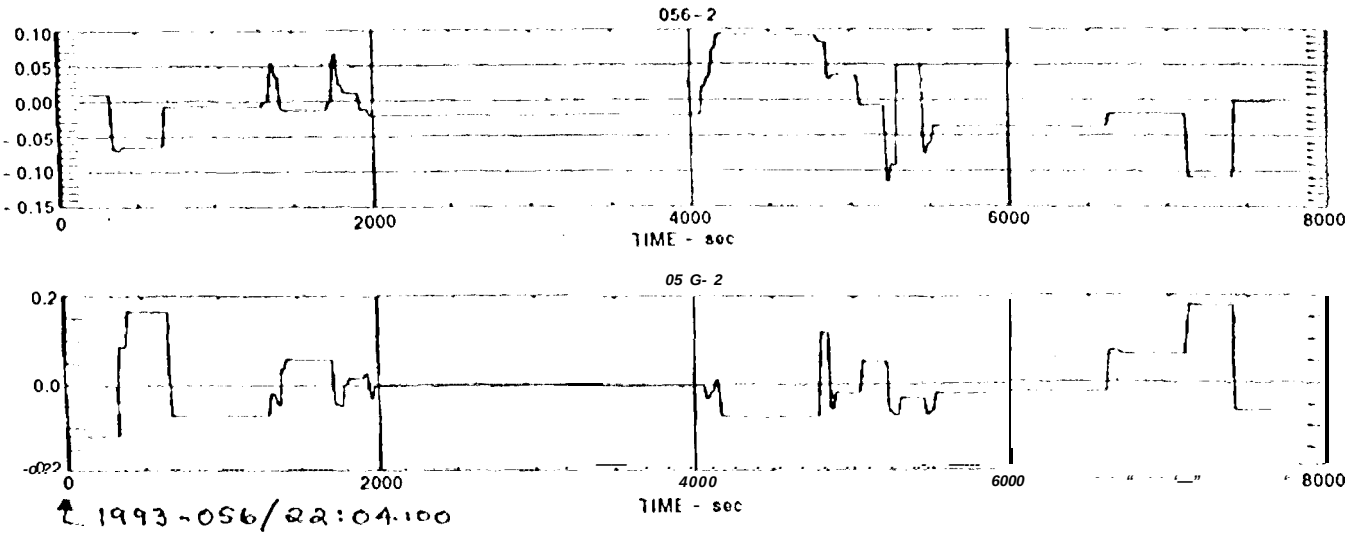

Fig. 9. Position accuracy: on-orbit results.

TOPEX/POSEIDON Star Tracker was < 0.17 magnitude based on traceability of the radiometer back to the National Institute of Standards and Technology (NISI') and other estimated calibration errors.

Figure 10 shows the mean magnitude error and 1o magnitude error versus mission day. Each point represents the statistics for all the stars the OBC identified for that day. Up to mission clay 128, December **16,1992,** many stars were rejected by the star identification filter due to a magnitude bias error. This skewed the statistics and initially raised some. concern since the bias error appeared to be increasing as a function of time. On mission day 128, a 0.25 magnitude offset was applied. This increased the number of stars identified and included in the magnitude error statistics.

Preliminary analysis of the data shows no correlation between the bias error and the color or magnitude of the star. Magnitude trending continues to determine if the bias error is time dependent. Prior to the anomaly the ASTRA-B sensor showed a similar bias error.q'his indicates a systematic error in the magnitude calibration of the sensors. The cause of this bias error has not yet been identified.

7.4. Magnitude stability error

Magnitude stability errors include both temporal anti spatial components. Temporal errors result from shot noise, both from signal and background, and from noise in the analog electronics. Spatial errors can be broken into low and high spatial frequency components. Over the sensor field of view the point spread function of the optics may change and nonlinear effects discussed earlier, saturation, truncation, and thresholding may cause field dependent variations in the reported magnitude. These same nonlinear effects can also cause magnitude variations which arc a function of pixel phasing. The percent energy in a pixel will change as the phasing, the position of the centroid relative to the. pixel center, changes."l"his can cause high spatial frequency variations in the reported magnitude with a spatial period of a pixel.

Figure 11 shows the variation in the reported magnitude of a star as the image was slewed cross the diagonal of the field of view at a line of sight (1 .0S) rate of 0.3 de.grce/second during acceptance testing. Figure 12 shows on-orbit data for a star moving across the sensor field of view. It is clear that there is a systematic error in the reported magnitude which is a function of field position. Field dependent errors appear to be the major stability error contributor. The magnitude dependency upon column position is not presented due to insufficient on-orbit data. However, based upon ground test data, it is believed to be similar to the row dependency presented in Fig. 11. In addition, due to differences in LOS rate and resulting image smear, the data presented in Figs. 11 and 12 arc not necessarily directly comparable..

7.S, Proton rejection capabilities

The effects of radiation-induced noise events on the CCD must be addressed for a star sensor to operate in a natural or enhanced radiation environment. A unique feature of the. ASTRA Star Tracker is its ability to operate in the presence of a

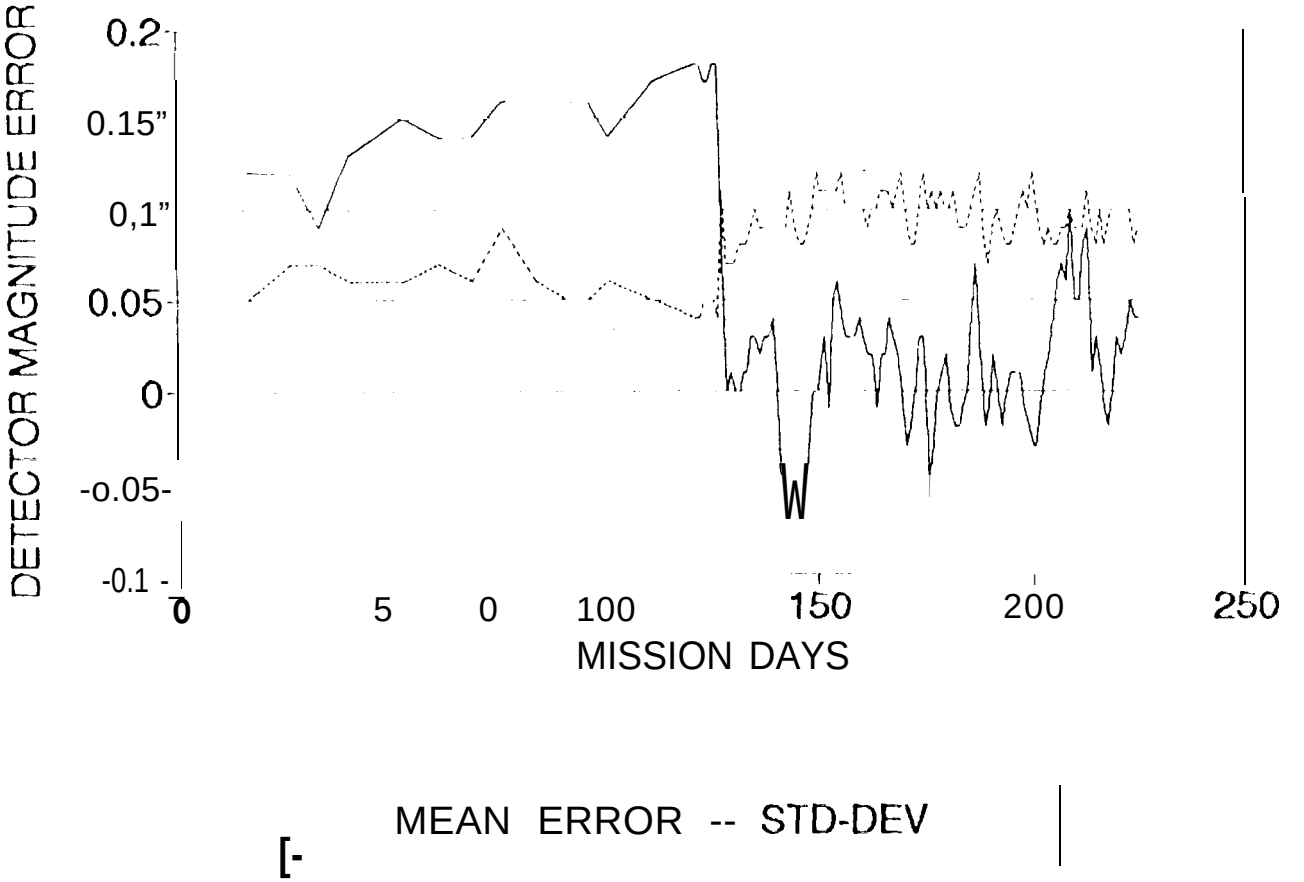

Fig. 10. Magnitude accuracy: on-orbit results.

large number of transient events[9]. As stated earlier, the TOPEX/POSEIDON operational orbit is such that the satellite must operate in the South Atlantic Anomaly (SAA) region for extended periods. In the. SAA, the flux of high energy protons and electrons trapped in the Earth's magnetic fields increases by orders of magnitude as was shown in Fig. 2. Charge.d particles interact directly with the CCD pixels, causing a random series of ionization events. These events can be localized to a fcw pixels or can result in long streaks, depending on the angle of incidence, the CCD geometry, and the particle's energy[10].

Transient events can degrade a star tracker's performance in a number of ways. During acquisition, transient events may be falsely acquired or may impede the acquisition of a valid star. During track, transient events can corrupt position and magnitude data or may result in the sensor dropping track on a valid star, A method to reduce the impact of these events on the sensor operation is required if the sensor is to operate ina high density proton environment. The most obvious solution is to increase the shielding around the CCD to reduce the number of events. However, this merely shifts the energy of the charged particles and will increase system size and weight. A more elegant solution is the application of real-time processing to reject these transient events.

For the. q'OI'IiXfl'OSI; IDONn~ission it was determined that the star tracker must operate with up to 1S0 transient events at the CCD pcr frame. The system had to meet the following requirements:

- Acquire and track stars with up to 1S0 transient events per frame
- 95% probability of acquiring a valid star within 22 seconds
- Identify and alert host if data has been corrupted by a transient event.

In order to demonstrate the transient event rejection algorithms during acceptance testing, a scene simulator was used, The scene simulator consisted of a CRT screen and a collimator which produced simulated star patterns along with

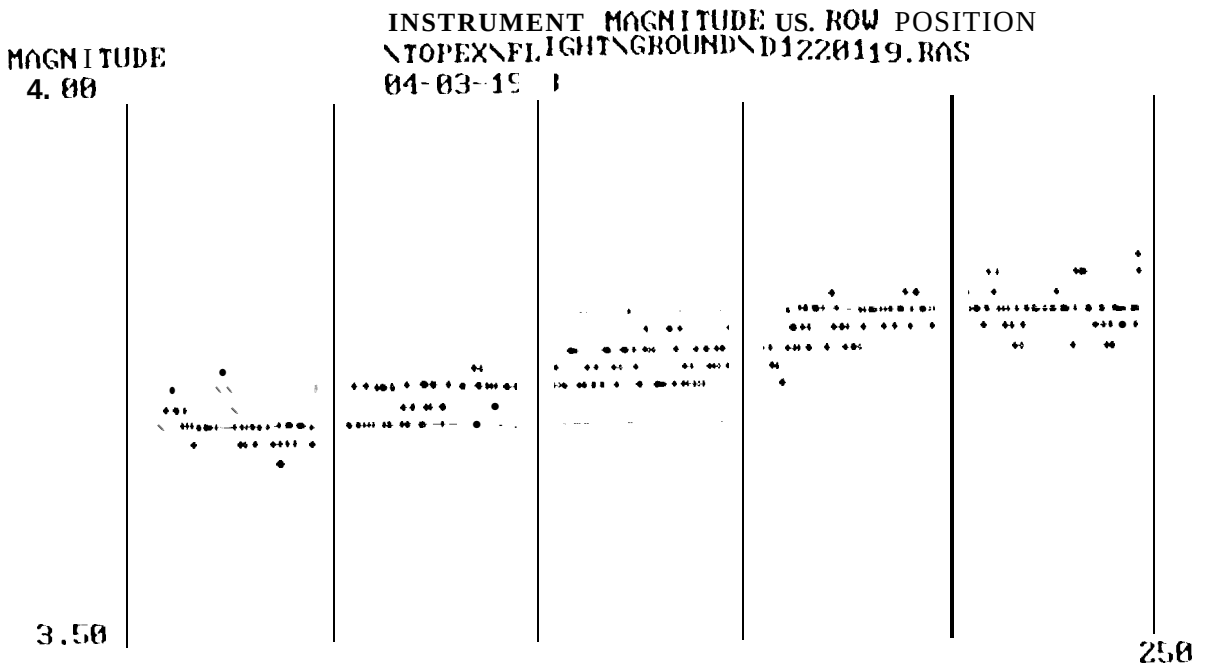

Fig. 11. Magnitude accuracy ground results.

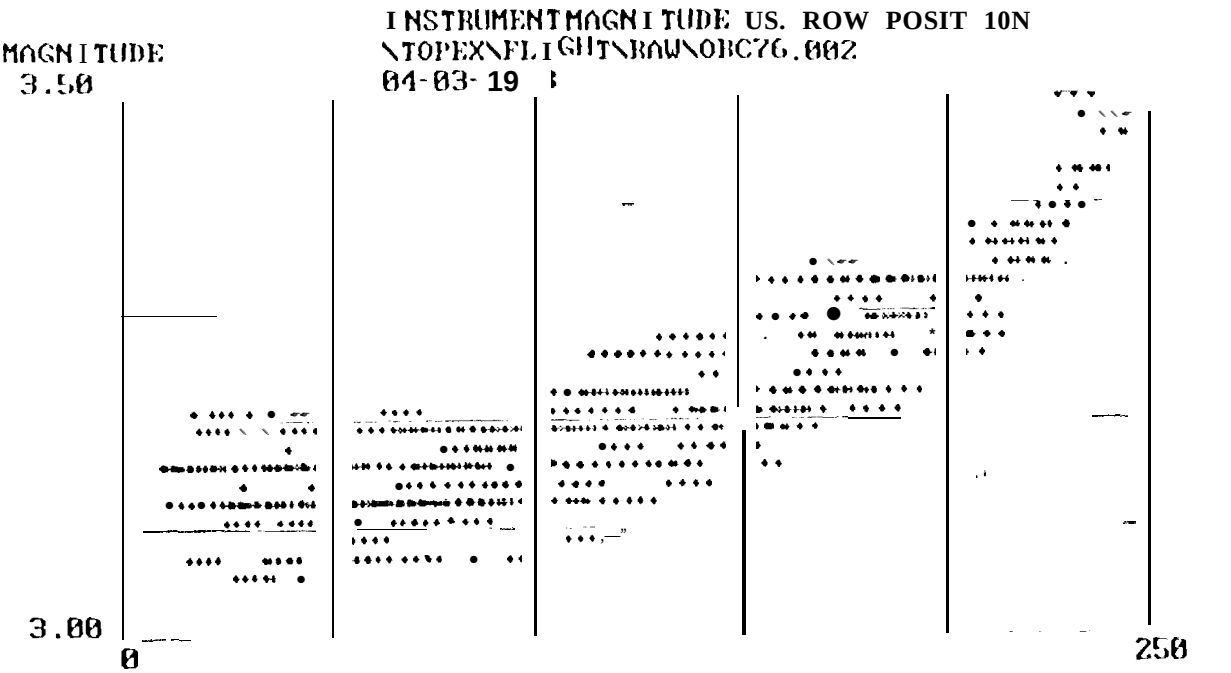

Fig. 12. **Magnitude accuracy:** on-orbit mulls.

transient events. The simulator was computer driven and produced a real-time, 10 Hz, input to the star tracker. Scenes were developed to test specific cases and to provide statistical data.

The transient rejection algorithm is based on the assumption that the position and magnitude of a star image will change systematically frame to frame, where transient events are completely random. Spatial and magnitude comparisons are used to determine if an image is valid. The far left plot on Fig. 13 shows effects of transient events on the reported position of a star using the ASTRA transient rejection algorithms. The center plot shows the reported position with the magnitude comparison filter disabled. Note that the frequency of the errors and the magnitude of the errors increases. The far right plot shows the reported position without transient rejection, the frequency and magnitude of the errors is greatly increased.

The following results were measured during the acceptance testing of the "1'01'1 :X/POSEIDON Star Trackers:

- No acquisition of transient events were observed
- Acquisition of valid stars within 7.11 sec average, 13.11 sec 3σ
- Successful identification of transient corrupted data
- No loss of track for valid stars.

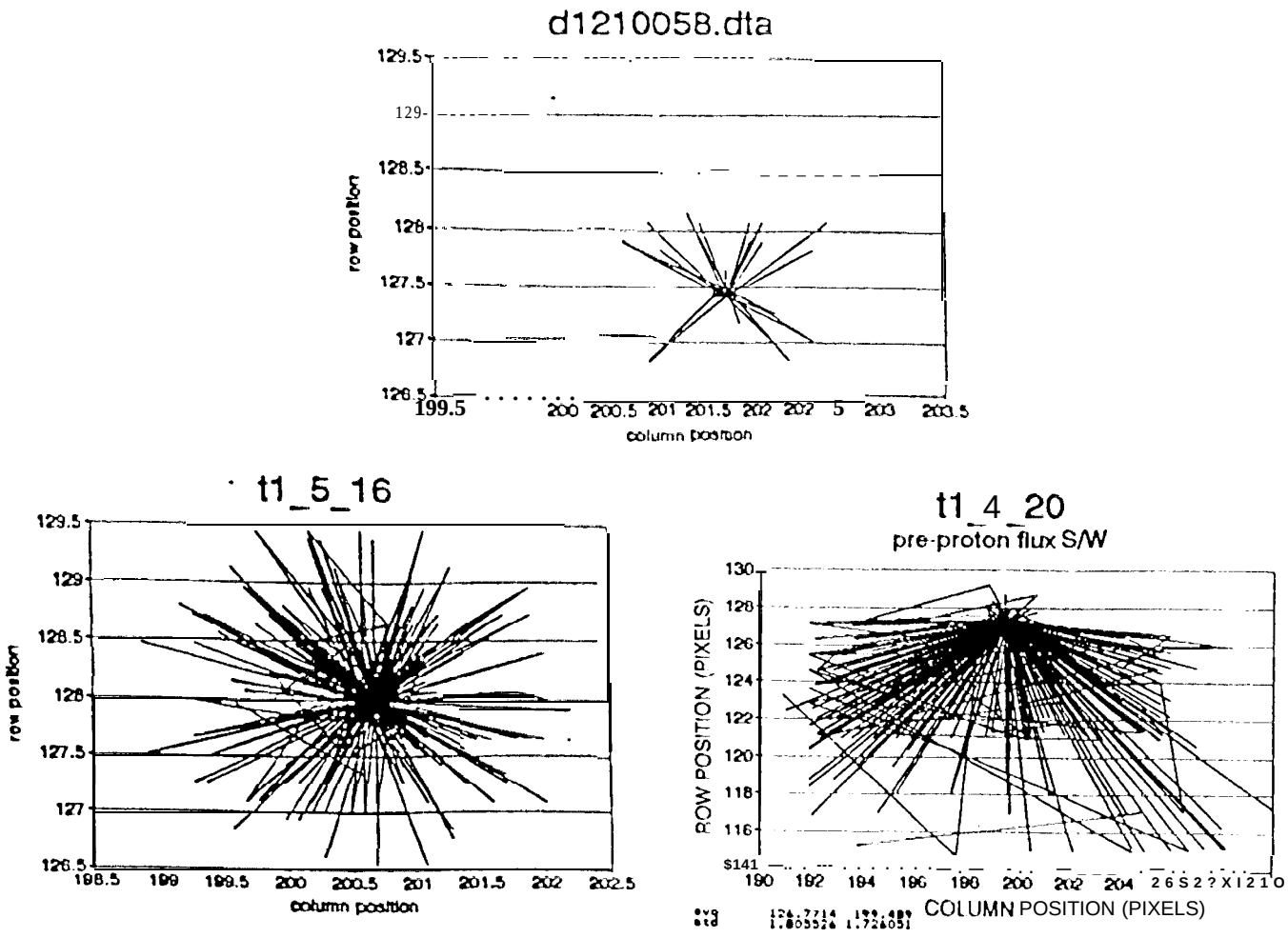

Fig. 13. Transient event discrimination: ground test results.

Preliminary analysis of the on-orbit data indicates that the ASTRA Star Tracker successfully acquires and tracks stars in the SAA. No performance degradation or anomalies of the star tracker has been observed while operating in the SAA. Recently "flex data format" which allows frame by frame analysis of the star tracker telemetry data has been made available. Further work is required in order to quantify the performance of the star tracker throughout the SAA.

8. CONCLUSIONS

- TOPEX/POSEIDON mission attitude determination objectives are being met
- Position accuracy reported by the star tracker is better than 40 arcsec peak
- Magnitude stability over the field of view is better than 0.22 magnitude 3σ
- Star tracker operates properly throughout SAA
- ASTRA-B is in an anomalous operating mode, potentially recoverable through power-cycling

9. ACKNOWLEDGMENT

The authors would like to thank the following for their assistance in providing data and information presented in this paper.

Paul Sanneman, Chuck Gay, and Ray Welch from Fairchild Space & Defense Corporation.

Allan Chow from Jet Propulsion Laboratory, California institute of Technology.

Frank Kissh, Bob McGuffy, and Rena Abreu from Hughes Danbury Optical Systems.

The research described in this paper was carded out by Hughes Danbury Optical Systems and the Jet Propulsion Laboratory, Call fornia Institute of Technology, under a contract with the National Aeronautics and Space Administration.

10. REFERENCES

1. "TOPEX/POSEIDON Project Mission Plan", JPL internal document D-6862 Rev. C, August, 1991.

2. R. J. Williams, C.J. Dennehy, D.Lee, R.V. Welch, "An Augmented MMS MACS for TOPEX/POSEIDON MissIon and Beyond" 1/19/90 AAS 90-013.

3. C.J. Dennehy, K. Ha, R.V. Welch, T. Kia, "On-Board Attitude Determination for TOPEX Satellite" AIAA 89-3622 August, 1989.

4. J. Janesick, T. Elliott, F. Pool, "Radiation Damage in Scientific CCD's" IEEE 1988 Nuclear Science Symposium, Orlando, FL.

5. C. Gay, R.V. Welch, V. Selby, "Living with On-Orbit Anomalies in the TOPEX/POSEIDON Earth Sensors" 2/6/93 AAS 934)44.

6. S. Davis, J. Lai, "Attitude Sensor Calibration for the Ocean Topography Experiment (TOPEX) Spacecraft" SPIE Space Guidance, Control, and Tracking Conference, Orlando, 1993.

7. D.J. Flynn "Ocean Topography Experiment (TOPEX) Star Tracker Performance" SPIE Acquisition, Tracking, and Pointing Conference, Orlando, 1992.

8. H.C. Strunz, T. Baker, D. Ethridge "Estimation of Stellar Magnitudes" SPIE Space Guidance, Control, and Tracking Conference, Orlando, 1993.

9. K-J. Miklus, F. Kissh, DJ. Flynn "Star Tracker Operation in a High Density Proton Field" GSFC Flight Mechanics/Estimation Theory Symposium, May, 1992.

10. F. Kubick "Statistical Aspects of CCD Radiation Noise" HDOS internal memo.